

Synthesis and X-ray Structures of a Series of Heteroleptic Selenites of Copper[†]

Antonio Sousa-Pedrares,^{*,‡} María Luz Durán,[‡] José Arturo García-Vázquez,[‡] Jaime Romero,[‡]
Antonio Sousa,[‡] and José A. Real[§]

Departamento de Química Inorgánica, Universidad de Santiago de Compostela, 15782 Santiago de Compostela, Spain, and Instituto de Ciencia Molecular/Departamento de Química Inorgánica, Universidad de Valencia, Edificio de Institutos de Paterna, P.O. Box 22085/47071, Valencia, Spain

Received October 8, 2008

The reactions of $[\text{Cu}(\text{R-pySe})]$, $\text{R} = \text{H}$, 3-CF_3 , with 2,2'-bipyridine or 1,10-phenanthroline in acetonitrile yielded the one-dimensional complexes $\{[\text{Cu}(\text{SeO}_3)(\text{phen})] \cdot 2(\text{H}_2\text{O})\}_n$, **1**, $\{[\text{Cu}(\text{SeO}_3)(\text{bipy})] \cdot 2(\text{H}_2\text{O})\}_n$, **2**. Recrystallization of **1** and **2** from a 1:1 methanol/water mixture led to the formation of the dinuclear complexes $[\text{Cu}(\text{SeO}_3)(\text{phen})(\text{H}_2\text{O})]_2$, **3**, and $[\text{Cu}(\text{SeO}_3)(\text{bipy})(\text{H}_2\text{O})]_2$, **4**. Single crystal X-ray diffraction analysis revealed that **1** and **2** have a polymeric structure in which each oxygen atom of the selenite group coordinates to a copper atom. The two other coordination positions are occupied by two nitrogen atoms of the organic ligand, and this defines an almost square pyramidal geometry around the metal. Both compounds show a very weak antiferromagnetic coupling ($J = -0.9$ for **1** and -0.6 cm^{-1} for **2**). Compounds **3** and **4** consist of dinuclear species with the copper atoms lying in a square pyramidal geometry in which the selenite group acts as a bridge between two copper atoms and one oxygen atom is uncoordinated. The two copper ions in **3** show antiferromagnetic coupling with $J = -22.1 \text{ cm}^{-1}$.

Introduction

The study of the crystal chemistry of low-dimensional compounds is an area of intense activity owing to their specific and often unusual properties. One way to obtain low-dimensional compounds is to use the so-called lone pair cations, which are believed to act as structural scissors. For this reason, a great deal of research is being carried out on inorganic materials containing oxy-anions of group 16 elements, such as Se(IV) and Te(IV).^{1–4} Structurally, compounds containing Se(IV) are also of interest because of the possible role of the lone pair of electrons as invisible structure-directing agents. In fact, the crystal chemistry of compounds containing selenite(IV) or tellurite(IV) groups

is characterized by the space requirement of the lone pair electrons, which causes them to be as far apart as possible.^{5,6} If the compound is a polymer, this requirement could produce compounds with low-dimensional arrangements in the crystal structure. In most cases these compounds are oxohalogenides comprising transition metals and elements such as Se(IV) or Te(IV).^{7–13} The lone-pair elements [Se(IV) or Te(IV)] and the halogens constitute “structural scissors” that hinder the development of the three-dimensional networks. In these kinds of oxohalogenide compounds, the lone-pair elements

[†] Dedicated to the memory of Prof. J. Strahler.

* To whom correspondence should be addressed. E-mail: antonio.sousa.pedrares. Phone: +34-981563100, ext. 14252. Fax: +34-981547102.

[‡] Universidad de Santiago de Compostela.

[§] Universidad de Valencia.

- (1) Xiao, D.; Wang, S.; Wang, E.; Hou, Y.; Li, Y. G.; Hu, C.; Xu, L. *J. Solid State Chem.* **2003**, *176*, 159–164.
- (2) Pasha, I.; Choudhury, A.; Rao, C. N. R. *Inorg. Chem.* **2003**, *42*, 409–415.
- (3) Xiao, D.; Li, Y.; Wang, E.; Wang, S.; Hou, Y.; De, G.; Hu, C. *Inorg. Chem.* **2003**, *42*, 7652–7657.
- (4) De, G.; Li, Y.; Huang, R.; Wang, E.; Yuan, M.; Hu, C.; Xu, L. *Inorg. Chem. Commun.* **2003**, *6*, 1091–1095.

- (5) Almond, P. M.; Albrecht-Schmitt, T. E. *Inorg. Chem.* **2002**, *41*, 5495–5501.
- (6) Johnston, M. G.; Harrison, W. T. A. *J. Am. Chem. Soc.* **2002**, *124*, 4576–4577.
- (7) Johnsson, M.; Lidin, S.; Törnroos, K. W.; Burgi, H.-B.; Millet, P. *Angew. Chem., Int. Ed.* **2004**, *43*, 4292–4295.
- (8) Becker, R.; Prester, M.; Berger, H.; Johnsson, M.; Drobac, D.; Zivkovic, I. *Solid State Sci.* **2007**, *9*, 223–230.
- (9) Becker, R.; Prester, M.; Berger, H.; Lin, P.-H.; Johnsson, M.; Drobac, D.; Zivkovic, I. *J. Solid State Chem.* **2007**, *180*, 1051–1059.
- (10) Becker, R.; Berger, H.; Johnsson, M.; Prester, M.; Marohnic, Z.; Miljak, M.; Herak, M. *J. Solid State Chem.* **2006**, *179*, 836–842.
- (11) Becker, R.; Johnsson, M.; Kremer, R.-K.; Lemmens, P. *J. Solid State Chem.* **2005**, *178*, 2024–2029.
- (12) Johnsson, M.; Törnroos, K. W.; Mila, F.; Millet, P. *Chem. Mater.* **2000**, *12*, 2853–2857.
- (13) Johnston, M.; Törnroos, K. W.; Lemmens, P.; Millet, P. *Chem. Mater.* **2003**, *15*, 68–73.

are coordinated only by oxygen and the metal ions are coordinated by both oxygen and halogens. For example, it was proposed that $\text{Cu}_2\text{TeO}_5\text{X}_2$ ($\text{X} = \text{Cl}, \text{Br}$),¹² which consists of tetrahedral clusters of Cu(II) linked by bridging Te–O units, is an example of a quasi-zero-dimensional system. Compounds with a general formula $\text{Ni}_5(\text{TeO}_3)_4\text{X}_2$ ($\text{X} = \text{Cl}, \text{Br}$)¹³ are layered structures with two-dimensional arrangements of NiO_6 and NiO_5X octahedra and TeO_3E tetrahedra. However, relatively little work has been done on the (M/X/O) systems ($\text{M} =$ transition metal, $\text{X} = \text{Se}$ or Te), and the crystal structures of a few compounds have been described, including $\text{M}^{2+}\text{SeO}_3$ ($\text{M} = \text{Co}, \text{Cu}$),¹⁴ CuTe_2O_5 ,¹⁵ and NiSeO_3 .¹⁶ In addition, it is noteworthy that the introduction of N-containing chelating bidentate ligands such as phen or bipy to the metal center may lead to novel structures. The ligand may thus serve to “passivate” the metal site through the N donors, which may adjust the dimensionality of these compounds.^{1–4,17} Many of these complexes have been obtained using hydrothermal methods.^{1–6}

In this paper we describe the reaction of $[\text{Cu}(3\text{-CF}_3\text{-pySe})]$ and $[\text{Cu}(\text{pySe})]$ in air with 1,10-phenanthroline and 2,2'-bipyridine in acetonitrile to prepare the one-dimensional chains $\{[\text{Cu}(\text{SeO}_3)(\text{phen})] \cdot 2(\text{H}_2\text{O})\}_n$, **1**, and the one-dimensional $\{[\text{Cu}(\text{SeO}_3)(\text{bipy})] \cdot 2(\text{H}_2\text{O})\}_n$, **2**. Recrystallization of **1** and **2** from a 1:1 methanol/water mixture yielded dinuclear complexes: $[\text{Cu}(\text{SeO}_3)(\text{phen})(\text{H}_2\text{O})]_2$, **3**, and $[\text{Cu}(\text{SeO}_3)(\text{bipy})(\text{H}_2\text{O})]_2$, **4**. The structures and magnetism of these compounds are also described.

Experimental Section

General Considerations. All solvents and 1,10-phenanthroline and 2,2'-bipyridine were commercial products and were used as supplied. Copper (Aldrich) was used as 2×2 cm plates. The syntheses of $(\text{pySe})_2$ and $(3\text{-CF}_3\text{-pySe})_2$ were carried out by reacting sodium diselenide with the appropriate 2-bromopyridine in dimethylformamide following a literature procedure.¹⁸ The precursor complexes $[\text{Cu}(3\text{-CF}_3\text{-pySe})]$ and $[\text{Cu}(\text{pySe})]$ were obtained using an electrochemical procedure, as described below.

Microanalyses were performed using a Perkin-Elmer 240B microanalyzer. IR spectra were recorded on a Perkin-Elmer 1330 spectrophotometer. Variable temperature magnetic susceptibility measurements were carried out on microcrystalline samples (5–20 mg) of compounds **1–4**, using a Quantum Design MPMS2 SQUID susceptometer equipped with a 5.5 T magnet, operating at 0.1–1 T and at temperatures from 300–1.8 K. The susceptometer was calibrated with $(\text{NH}_4)_2\text{Mn}(\text{SO}_4)_2 \cdot 12\text{H}_2\text{O}$. Experimental susceptibilities were corrected for diamagnetism of the constituent atoms by the use of Pascal's constants.

Synthesis of Copper Precursors. The complexes $[\text{Cu}(3\text{-CF}_3\text{-pySe})]$ and $[\text{Cu}(\text{pySe})]$ were obtained using an electrochemical

procedure.¹⁹ The cell was a 100 mL tall-form beaker fitted with a rubber bung. An acetonitrile solution of the diselenide containing tetraethylammonium perchlorate (10 mg) was electrolyzed using a platinum wire as the cathode and a copper plate as a sacrificial anode suspended from another platinum wire (**Caution! Perchlorate compounds are potentially explosive and should be handled in small quantities and with great care**). The cells can be summarized as: $\text{Cu}_{(+)} / \text{CH}_3\text{CN} + (\text{R-pySe})_2 / \text{Pt}_{(-)}$, $\text{R} = \text{H}, 3\text{-CF}_3$.

Synthesis of $[\text{Cu}(\text{pySe})]$. Electrochemical oxidation under nitrogen of a copper anode in a solution of 2,2'-bis(pyridyl) diselenide, $(\text{pySe})_2$, (0.117 g, 0.373 mmol) in acetonitrile (50 mL) at 7 V and 10 mA for 2 h caused 46 mg of copper to be dissolved ($E_f = 0.97 \text{ mol} \cdot \text{F}^{-1}$). During the electrolysis, the color of the solution changed from dark yellow to green, and a dark green precipitate appeared. The solid was filtered, washed with diethyl ether and air-dried. The elemental analysis data for the solid are consistent with the proposed formula. Anal. Found (Calcd) for $\text{C}_5\text{H}_4\text{NSeCu}$: C, 27.1 (27.2); H, 1.8 (1.8); N, 6.4 (6.3)%.

Synthesis of $[\text{Cu}(3\text{-CF}_3\text{-pySe})]$. Electrochemical oxidation under nitrogen of a copper anode in a solution of 2,2'-bis(3-trifluoromethylpyridyl) diselenide, $(3\text{-CF}_3\text{-pySe})_2$, (0.168 g, 0.373 mmol) in acetonitrile (50 mL) at 6 V and 10 mA for 2 h caused 45 mg of copper to be dissolved ($E_f = 0.95 \text{ mol} \cdot \text{F}^{-1}$). During the electrolysis, the color of the solution changed from dark yellow to red, and a red precipitate appeared. The solid was filtered, washed with diethyl ether, and air-dried. The elemental analysis data for the solid are consistent with the proposed formula. Anal. Found (Calcd) for $\text{C}_6\text{H}_3\text{F}_3\text{NSeCu}$: C, 25.4 (25.0); H, 1.1 (1.1); N, 4.9 (4.9)%.

Synthesis of $\{[\text{Cu}(\text{SeO}_3)(\text{phen})]\}_n$ (1**).** When the non-filtered reaction mixture of $[\text{Cu}(3\text{-CF}_3\text{-pySe})]$ is left to stir overnight in air in the presence of 1,10-phenanthroline (phen) (0.134 g, 0.746 mmol), it gradually changes from red to green and a light green precipitate appears. The solid was filtered, washed with diethyl ether, and air-dried. Yield: 0.167 g (90.9%). The elemental analysis for the solid is consistent with the formula of the monohydrate $\{[\text{Cu}(\text{SeO}_3)(\text{phen})] \cdot (\text{H}_2\text{O})\}_n$. Anal. Found (Calcd) for $\text{C}_{12}\text{H}_{10}\text{N}_2\text{O}_4\text{SeCu}$: C, 37.1 (37.0); H, 2.6 (2.6); N, 7.5 (7.2)%. IR (KBr, cm^{-1}): 3414br, 3057w, 1671w, 1618m, 1582m, 1561m, 1517s, 1494m, 1427s, 1404s, 1369m, 1340m, 1316s, 1225w, 1165m, 1143m, 1110s, 1059w, 1040w, 1024m, 909w, 872m, 849s, 806w, 770m, 723vs, 647w, 495w.

Single crystals of compound (**1**) could be obtained from the mother liquor. X-ray analysis revealed that the crystallized compound was the dihydrate $\{[\text{Cu}(\text{SeO}_3)(\text{phen})] \cdot 2(\text{H}_2\text{O})\}_n$.

The same compound is obtained when the reaction mixture of $[\text{Cu}(\text{pySe})]$ is used.

Synthesis of $\{[\text{Cu}(\text{SeO}_3)(\text{bipy})]\}_n$ (2**).** Compound (**2**) was obtained in a similar way as (**1**), by stirring overnight the non-filtered reaction mixture of $[\text{Cu}(3\text{-CF}_3\text{-pySe})]$ in air in the presence of 2,2'-bipyridine (bipy) (0.116 g, 0.746 mmol). The reaction yields 0.134 g (81.7%) of a light green solid. The elemental analysis for the solid is consistent with the formula $\{[\text{Cu}(\text{SeO}_3)(\text{phen})]\}_n$. Anal. Found (Calcd) for $\text{C}_{10}\text{H}_8\text{N}_2\text{O}_3\text{SeCu}$: C, 34.8 (34.6); H, 2.8 (2.3); N, 8.3 (8.1)%. IR (KBr, cm^{-1}): 3432br, 3079w, 1680w, 1619s, 1553m, 1529s, 1476m, 1447s, 1405w, 1368w, 1316s, 1273w, 1254w, 1175m, 1160s, 1123s, 1112s, 1070w, 1041s, 969w, 886w, 808m, 771vs, 732s, 703s, 672m, 637w, 503w, 419w.

Single crystals of compound (**2**) could be obtained from the mother liquor. X-ray analysis revealed that the crystallized com-

(14) Kohn, K.; Inoue, K.; Horie, O.; Akimoto, S.-I. *J. Solid State Chem.* **1976**, *18*, 27–37.

(15) Deisenhofer, J.; Eremina, R. M.; Pimenov, A.; Gavrilova, T.; Berger, H.; Johnsson, M.; Lemmens, P.; Krug von Nidda, H.-A.; Loidl, A.; Lee, K.-S.; Whangbo, M.-H. *Phys. Rev.* **2006**, *74* B, 174421/1–174421/8.

(16) Miljak, M.; Becker, R.; Herak, M.; Prester, M.; Milat, O.; Johnsson, M.; Berger, H. *J. Phys.: Condens. Matter* **2007**, *19*, 196203/1–196203/14.

(17) Li, Y.; Wang, E. B.; Zhang, H.; Luan, G.; Hu, C. W. *J. Solid State Chem.* **2002**, *163*, 10–16.

(18) Brandsma, L.; Wijers, H. E. *Rec. Trav. Chim. Pays Bas* **1963**, *82*, 68–74.

(19) García-Vázquez, J. A.; Romero, J.; Sousa, A. *Coord. Chem. Rev.* **1999**, *193–195*, 691–745.

Table 1. Summary of Crystallographic Data and Refinement for Copper Compounds

compound	1	2	3	4	5
empirical formula	C ₁₂ H ₁₂ CuN ₂ O ₅ Se	C ₁₀ H ₁₂ CuN ₂ O ₅ Se	C ₂₄ H ₃₆ Cu ₂ N ₄ O ₁₆ Se ₂	C ₁₀ H ₁₄ CuN ₂ O ₆ Se	C ₂₂ H ₁₆ CuF ₆ N ₄ O ₃
formula weight	406.74	382.72	921.57	400.73	561.93
crystal size, mm	0.55 × 0.20 × 0.20	0.13 × 0.04 × 0.03	0.27 × 0.20 × 0.14	0.51 × 0.26 × 0.22	0.30 × 0.23 × 0.14
temperature, K	293(2)	120(2)	120(2)	293(2)	293(2)
wavelength	0.71073	0.71073	0.71073	0.71073	0.71073
crystal system	monoclinic	monoclinic	triclinic	triclinic	monoclinic
space group	C2/c	C2/c	P1	P1	P2(1)/n
Unit cell dimens.					
a, Å	19.7502(5)	16.634(3)	7.3902(14)	8.037(2)	7.2325(15)
b, Å	14.0656(3)	13.812(2)	10.1998(19)	8.792(2)	18.721(4)
c, Å	11.1977(3)	11.169(2)	11.492(2)	10.337(3)	16.265(3)
α/deg	90.00	90.00	99.345(3)	73.551(4)	90.00
β/deg	104.1590(10)	102.494(3)	94.413(3)	89.148(4)	92.639(4)
γ/deg	90.00	90.00	110.329(3)	74.841(4)	90.00
volume, Å ³	3016.20(13)	2505.1(8)	793.1(3)	674.8(3)	2200.0(8)
Z	8	8	1	2	4
μ, mm ⁻¹	3.882	4.667	3.716	4.341	1.078
no. reflections collected	10170	10476	9274	7864	25124
no. of independent reflections	3702	2565	3370	2966	4506
	[R(int) = 0.0546]	[R(int) = 0.0983]	[R(int) = 0.0281]	[R(int) = 0.0261]	[R(int) = 0.0398]
data/restraints/parameters	3702/ 6/206	2565/ 0/185	3370/ 2/255	2966/ 0/205	4506/ 0/333
goodness-of-fit	0.971	0.942	1.075	1.056	1.069
final R indices [I > 2σ(I)]	R = 0.0663	R = 0.0499	R = 0.0249	R = 0.0273	R = 0.0370
	Rw = 0.1594	Rw = 0.1080	Rw = 0.0680	Rw = 0.0674	Rw = 0.0931

pound was the dihydrate $\{[\text{Cu}(\text{SeO}_3)(\text{bipy})] \cdot 2(\text{H}_2\text{O})\}_n$. The same compound is obtained when the reaction mixture of $[\text{Cu}(\text{pySe})]$ is used.

After aerial oxidation of $[\text{Cu}(3\text{-CF}_3\text{-pySe})]$ in the presence of bipy, crystals of a different compound (**5**) were isolated. X-ray analysis of these crystals revealed they have the formula $[\text{Cu}(3\text{-CF}_3\text{-pyO})_2(\text{bipy})(\text{H}_2\text{O})]$.

Synthesis of $[\text{Cu}(\text{SeO}_3)(\text{phen})(\text{H}_2\text{O})]_2$ (3**).** Compound (**3**) was quantitatively obtained by crystallization of $\{[\text{Cu}(\text{SeO}_3)(\text{phen})] \cdot (\text{H}_2\text{O})\}_n$, (**1**) from a 1:1 methanol/water mixture. The compound was obtained as green crystals. The elemental analysis data for the crystals are consistent with the formula of the hydrate $[\text{Cu}(\text{SeO}_3)(\text{phen})(\text{H}_2\text{O})]_2 \cdot 8(\text{H}_2\text{O})$. Anal. Found (Calcd) for **3** C₂₄H₃₆N₄O₁₆Se₂Cu₂: C, 32.8 (31.3); H, 3.2 (3.9); N, 6.5 (6.1) %. IR (KBr, cm⁻¹): 3442br, 3084w, 1626m, 1608w, 1586m, 1517m, 1494w, 1427s, 1347w, 1318w, 1224w, 1200w, 1143w, 1121m, 1109m, 1047w, 856s, 766s, 724vs, 647w, 518w, 499w, 426w.

Synthesis of $[\text{Cu}(\text{SeO}_3)(\text{bipy})(\text{H}_2\text{O})]_2$ (4**).** Crystallization of $\{[\text{Cu}(\text{SeO}_3)(\text{phen})]\}_n$, (**2**), from a 1:1 methanol/water mixture yields (**4**) as blue crystals. The elemental analysis data for the crystals are consistent with the formula $[\text{Cu}(\text{SeO}_3)(\text{phen})(\text{H}_2\text{O})]_2 \cdot 4(\text{H}_2\text{O})$. Anal. Found (Calcd) for **4** C₂₀H₂₈N₄O₁₂Se₂Cu₂: C, 27.2 (29.9); H, 3.1 (3.4); N, 6.4 (6.9) %. IR (KBr, cm⁻¹): 3423br, 3282br, 3107w, 3027w, 1657w, 1602m, 1566w, 1494w, 1473w, 1447m, 1315w, 1255w, 1159w, 1056w, 1031w, 812m, 774s, 734vs, 661w, 527w, 473w, 416w.

X-ray Crystallographic Studies. Intensity data for all compounds were collected using a Smart-CCD-1000 Bruker diffractometer (Mo K α radiation, $\lambda = 0.71073$ Å) equipped with a graphite monochromator. $\{[\text{Cu}(\text{SeO}_3)(\text{phen})] \cdot 2(\text{H}_2\text{O})\}_n$, $[\text{Cu}(\text{SeO}_3)(\text{bipy})(\text{H}_2\text{O})]_2$, and $[\text{Cu}(3\text{-CF}_3\text{-py-2-O})_2(\text{bipy})(\text{H}_2\text{O})]$ were measured at 293 K; Data for $\{[\text{Cu}(\text{SeO}_3)(\text{bipy})] \cdot 2(\text{H}_2\text{O})\}_n$ and $[\text{Cu}(\text{SeO}_3)(\text{phen})(\text{H}_2\text{O})]_2$ were collected at 120 K. The ω scan technique was employed to measure intensities in all crystals. Decomposition of the crystals did not occur during data collection. The intensities of all data sets were corrected for Lorentz and polarization effects. Absorption effects in all compounds were corrected using the program SADABS.²⁰ The crystal structures of all compounds were solved by direct methods. Crystallographic programs used for structure solution and refinement were those in SHELX97.²¹

Scattering factors were those provided with the SHELX program system. Missing atoms were located in the difference Fourier map and included in subsequent refinement cycles. The structures were refined by full-matrix least-squares refinement on F², using anisotropic displacement parameters for all non-hydrogen atoms. Hydrogen atoms not involved in hydrogen bonding were placed geometrically and refined using a riding model with U_{iso} constrained at 1.2 times U_{eq} of the carrier C atom.

Pertinent details of the data collections and structure refinements are given in Table 1, while important geometrical data for all compounds are listed in Tables 2–6.

Further details regarding the data collections, structure solutions, and refinements are included in the Supporting Information. Ortep3 drawings²² with the numbering scheme used are shown in Figures 2a, 3, 5, 6 and 9.

Crystallographic data (excluding structure factors) for the structures reported in this paper have been deposited with the Cambridge Crystallographic Data Centre as supplementary publication nos. CCDC 696202–696206 [1, 2, 3, 4, and 5]. Copies of the data can be obtained free of charge on application to CCDC, 12 Union Road, Cambridge CB21EZ, UK (fax: (44) 1223–336–033; e-mail: deposit@ccdc.cam.ac.uk).

Results and Discussion

As part of a program aiming to prepare copper compounds containing selenium, a series of 2-selenol pyridine copper compounds have been prepared. Unfortunately, many of these compounds could not be crystallized because of their polymeric nature, which results from the tendency of selenium to act as a bridge. To avoid this polymer formation, we attempted to block some of the coordination sites of copper by stirring the polymer in air with an acetonitrile

(20) Sheldrick, G. M. SADABS: Program for absorption correction using area detector data. University of Göttingen, Germany, 1996.

(21) Sheldrick, G. M. SHELX97 [Includes SHELXS97, SHELXL97, CIFT-AB] - Programs for Crystal Structure Analysis, Release 97-2; Institut für Anorganische Chemie der Universität: Tammanstrasse 4, D-3400 Göttingen, Germany, 1998.

(22) Farrugia, L. J. *J. Appl. Crystallogr.* **1997**, *30*, 565.

Table 2. Selected Bond Lengths [Å] and Angles [deg] for $\{[\text{Cu}(\text{SeO}_3)(\text{phen})] \cdot 2(\text{H}_2\text{O})\}_n$ (**1**)

Cu(1)–O(1)	1.934(3)	Cu(1)–O(2) ^{#1}	1.986(4)
Cu(1)–N(2)	2.022(4)	Cu(1)–N(1)	2.040(5)
Cu(1)–O(3) ^{#2}	2.349(4)	Se(1)–O(3)	1.667(3)
Se(1)–O(1)	1.700(4)	Se(1)–O(2)	1.722(4)
O(2)–Cu(1) ^{#1}	1.986(4)	O(3)–Cu(1) ^{#2}	2.349(4)
N(1)–C(1)	1.343(7)	N(1)–C(5)	1.357(6)
N(2)–C(10)	1.319(8)	N(2)–C(6)	1.360(8)
O(1)–Cu(1)–O(2) ^{#1}	97.78(16)	O(1)–Cu(1)–N(2)	165.48(19)
O(2) ^{#1} –Cu(1)–N(2)	94.07(19)	O(1)–Cu(1)–N(1)	85.64(16)
O(2) ^{#1} –Cu(1)–N(1)	165.91(17)	N(2)–Cu(1)–N(1)	80.9(2)
O(1)–Cu(1)–O(3) ^{#2}	92.45(14)	O(2) ^{#1} –Cu(1)–O(3) ^{#2}	97.26(14)
N(2)–Cu(1)–O(3) ^{#2}	94.36(16)	N(1)–Cu(1)–O(3) ^{#2}	96.24(16)
O(3)–Se(1)–O(1)	101.70(17)	O(3)–Se(1)–O(2)	103.9(2)
O(1)–Se(1)–O(2)	97.96(18)		

Hydrogen Bonds for **1** [Å and deg]

D–H···A	d(D–H)	d(H···A)	d(D···A)	<(DHA)
O(1S)–H(1SB)···O(2)	0.80(2)	1.98(5)	2.721(7)	153(10)
O(1S)–H(1SA)···O(3) ^{#3}	0.80(2)	2.28(10)	2.826(7)	126(11)
O(2S)–H(2SA)···O(1S)	0.81(2)	2.27(7)	2.979(11)	147(11)
O(2S)–H(2SB)···O(1S) ^{#4}	0.81(2)	2.15(5)	2.871(11)	148(8)

^{#1} Symmetry transformations used to generate equivalent atoms: $-x + 1, y, -z + 1/2$. ^{#2} Symmetry transformations used to generate equivalent atoms: $-x + 1, -y, -z + 1$. ^{#3} Symmetry transformations used to generate equivalent atoms: $x, -y, z - 1/2$. ^{#4} Symmetry transformations used to generate equivalent atoms: $-x + 1/2, -y + 1/2, -z$.

Table 3. Selected Bond Lengths [Å] and Angles [deg] for $\{[\text{Cu}(\text{SeO}_3)(\text{bipy})] \cdot 2(\text{H}_2\text{O})\}_n$ (**2**)

Cu(1)–O(1)	1.946(4)	Cu(1)–O(2) ^{#1}	1.986(5)
Cu(1)–N(2)	1.991(6)	Cu(1)–N(1)	2.020(6)
Cu(1)–O(3) ^{#2}	2.353(4)	Se(1)–O(3)	1.672(4)
Se(1)–O(2)	1.707(4)	Se(1)–O(1)	1.711(4)
O(2)–Cu(1) ^{#1}	1.986(5)	O(3)–Cu(1) ^{#2}	2.353(4)
O(1)–Cu(1)–O(2) ^{#1}	94.77(19)	O(1)–Cu(1)–N(2)	170.6(2)
O(2) ^{#1} –Cu(1)–N(2)	93.2(2)	O(1)–Cu(1)–N(1)	90.2(2)
O(2) ^{#1} –Cu(1)–N(1)	163.1(2)	N(2)–Cu(1)–N(1)	80.7(2)
O(1)–Cu(1)–O(3) ^{#2}	89.04(17)	O(2) ^{#1} –Cu(1)–O(3) ^{#2}	101.55(17)
N(2)–Cu(1)–O(3) ^{#2}	94.20(19)	N(1)–Cu(1)–O(3) ^{#2}	94.68(19)
O(3)–Se(1)–O(2)	103.4(2)	O(3)–Se(1)–O(1)	100.8(2)
O(2)–Se(1)–O(1)	97.7(2)		

Hydrogen Bonds for **2** [Å and deg]

D–H···A	d(D–H)	d(H···A)	d(D···A)	<(DHA)
O(1S)–H(1SA)···O(2)	0.75(8)	2.08(9)	2.744(7)	148(9)
O(1S)–H(1SB)···O(3) ^{#3}	0.92(9)	1.91(9)	2.784(7)	157(7)
O(2S)–H(2SA)···O(1S)	0.77(9)	2.11(9)	2.838(8)	159(10)
O(2S)–H(2SB)···O(1S) ^{#4}	0.84(9)	2.04(10)	2.863(9)	167(9)

^{#1} Symmetry transformations used to generate equivalent atoms: $-x, y, -z + 1/2$. ^{#2} Symmetry transformations used to generate equivalent atoms: $-x, -y, -z$. ^{#3} Symmetry transformations used to generate equivalent atoms: $x, -y, z + 1/2$. ^{#4} Symmetry transformations used to generate equivalent atoms: $-x + 1/2, -y + 1/2, -z + 1$.

solution of an ancillary ligand such as 1,10-phenanthroline or 2,2'-bipyridine. The aim of this process was to obtain oligomers that could be crystallized. $[\text{Cu}(3\text{-CF}_3\text{-pySe})]_n$ was chosen as the copper precursor for two reasons.

(a) The CF_3 group could act as a probe for NMR studies in cases where the isolated compound was soluble.

(b) Our previous experience shows that such a group provides crystallinity in the compounds.

However, the reaction with 1,10-phenanthroline (phen) did not produce the expected product but produced a compound that was shown by analytical data and X-ray structure to be $\{[\text{Cu}(\text{SeO}_3)(\text{phen})] \cdot 2(\text{H}_2\text{O})\}_n$, **1**. When **1**

Table 4. Selected Bond Lengths [Å] and Angles [deg] for $[\text{Cu}(\text{SeO}_3)(\text{phen})(\text{H}_2\text{O})]_2 \cdot 4\text{H}_2\text{O}$ (**3**)

Cu(1)–O(1)	1.9341(16)	Cu(1)–O(2) ^{#1}	1.9633(16)
Cu(1)–N(1)	2.0206(19)	Cu(1)–N(2)	2.023(2)
Cu(1)–O(4)	2.2613(19)	Se(1)–O(3)	1.6718(17)
Se(1)–O(1)	1.7054(16)	Se(1)–O(2)	1.7179(16)
O(2)–Cu(1) ^{#1}	1.9633(17)		
O(1)–Cu(1)–O(2) ^{#1}	95.37(7)	O(1)–Cu(1)–N(1)	171.22(7)
O(2) ^{#1} –Cu(1)–N(1)	93.39(7)	O(1)–Cu(1)–N(2)	89.71(7)
O(2) ^{#1} –Cu(1)–N(2)	161.69(7)	N(1)–Cu(1)–N(2)	81.74(8)
O(1)–Cu(1)–O(4)	89.81(8)	O(2) ^{#1} –Cu(1)–O(4)	102.80(7)
N(1)–Cu(1)–O(4)	88.90(8)	N(2)–Cu(1)–O(4)	94.78(7)
O(3)–Se(1)–O(1)	100.03(8)	O(3)–Se(1)–O(2)	102.87(8)
O(1)–Se(1)–O(2)	100.72(8)		

Hydrogen Bonds for **3** [Å and deg]

D–H···A	d(D–H)	d(H···A)	d(D···A)	<(DHA)
O(4)–H(4A)···O(3S)	0.70(3)	2.22(3)	2.893(3)	161(4)
O(4)–H(4B)···O(3S) ^{#2}	0.74(3)	2.08(3)	2.810(3)	174(3)
O(1S)–H(1SA)···O(3)	0.69(4)	2.07(4)	2.756(3)	170(4)
O(1S)–H(1SB)···O(3) ^{#3}	0.76(4)	2.11(4)	2.813(3)	155(3)
O(2S)–H(2SA)···O(1)	0.78(3)	2.09(4)	2.841(3)	164(3)
O(2S)–H(2SB)···O(1S) ^{#4}	0.77(3)	2.12(3)	2.841(3)	157(3)
O(3S)–H(3SA)···O(2)	0.93(6)	1.98(6)	2.824(3)	149(5)
O(3S)–H(3SB)···O(1S) ^{#4}	0.71(4)	2.07(4)	2.768(3)	166(4)
O(4S)–H(4SA)···O(2S)	0.882(18)	1.936(19)	2.817(3)	178(4)
O(4S)–H(4SB)···O(3) ^{#4}	0.874(18)	2.12(2)	2.985(3)	171(3)

^{#1} Symmetry transformations used to generate equivalent atoms: $-x + 1, -y + 1, -z$. ^{#2} Symmetry transformations used to generate equivalent atoms: $-x, -y + 1, -z$. ^{#3} Symmetry transformations used to generate equivalent atoms: $-x + 2, -y + 2, -z$. ^{#4} Symmetry transformations used to generate equivalent atoms: $x - 1, y, z$.

Table 5. Selected Bond Lengths [Å] and Angles [deg] for $[\text{Cu}(\text{SeO}_3)(\text{bipy})(\text{H}_2\text{O})]_2 \cdot 2\text{H}_2\text{O}$ (**4**)

Cu(1)–O(1)	1.9229(19)	Cu(1)–O(2) ^{#1}	1.9482(19)
Cu(1)–N(1)	2.019(2)	Cu(1)–N(2)	2.031(2)
Cu(1)–O(4)	2.317(2)	Se(1)–O(3)	1.6641(19)
Se(1)–O(1)	1.6922(19)	Se(1)–O(2)	1.711(2)
O(2)–Cu(1) ^{#1}	1.9482(19)		
O(1)–Cu(1)–O(2) ^{#1}	95.30(8)	O(1)–Cu(1)–N(1)	88.70(8)
O(2) ^{#1} –Cu(1)–N(1)	174.39(8)	O(1)–Cu(1)–N(2)	163.24(9)
O(2) ^{#1} –Cu(1)–N(2)	95.40(8)	N(1)–Cu(1)–N(2)	79.84(9)
O(1)–Cu(1)–O(4)	104.57(9)	O(2) ^{#1} –Cu(1)–O(4)	89.49(8)
N(1)–Cu(1)–O(4)	93.31(8)	N(2)–Cu(1)–O(4)	88.39(9)
O(3)–Se(1)–O(1)	100.93(10)	O(3)–Se(1)–O(2)	101.48(10)
O(1)–Se(1)–O(2)	101.36(10)		

Hydrogen Bonds for **4** [Å and deg]

D–H···A	d(D–H)	d(H···A)	d(D···A)	<(DHA)
O(1S)–H(1A)···O(3)	0.79(5)	1.92(5)	2.702(3)	169(5)
O(1S)–H(1B)···O(3) ^{#2}	0.79(4)	2.04(4)	2.817(4)	168(4)
O(2S)–H(2A)···O(2)	0.87(4)	1.98(4)	2.845(3)	173(4)
O(2S)–H(2B)···O(1S) ^{#3}	0.69(3)	2.23(4)	2.911(4)	173(4)
O(4)–H(4A)···O(1S) ^{#4}	0.81(4)	1.96(4)	2.742(3)	162(4)
O(4)–H(4B)···O(2S) ^{#5}	0.81(4)	1.97(4)	2.774(3)	172(3)

^{#1} Symmetry transformations used to generate equivalent atoms: $-x + 2, -y + 1, -z + 1$. ^{#2} Symmetry transformations used to generate equivalent atoms: $-x + 3, -y, -z + 1$. ^{#3} Symmetry transformations used to generate equivalent atoms: $x, y + 1, z$. ^{#4} Symmetry transformations used to generate equivalent atoms: $-x + 2, -y, -z + 1$. ^{#5} Symmetry transformations used to generate equivalent atoms: $x - 1, y, z$.

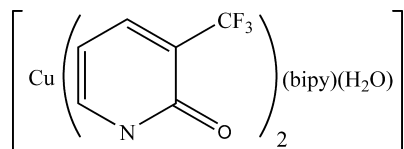
was crystallized from a 1:1 $\text{H}_2\text{O}/\text{CH}_3\text{OH}$ mixture, the new compound $[\text{Cu}(\text{SeO}_3)(\text{phen})(\text{H}_2\text{O})]_2$ was obtained, **3**. Similar compounds, $[\text{Cu}(\text{SeO}_3)(\text{bipy})] \cdot 2(\text{H}_2\text{O})_n$, **2**, and $[\text{Cu}(\text{SeO}_3)(\text{bipy})(\text{H}_2\text{O})]_2$, **4**, were isolated when 2,2'-bipyridine was used.

During the experiments with 2,2'-bipyridine (bipy), compound **5** was isolated as a byproduct (Figure 1).

Table 6. Bond Lengths [Å] and Angles [deg] for [Cu(3-CF₃-pyO)₂(bipy)(H₂O)] (5)

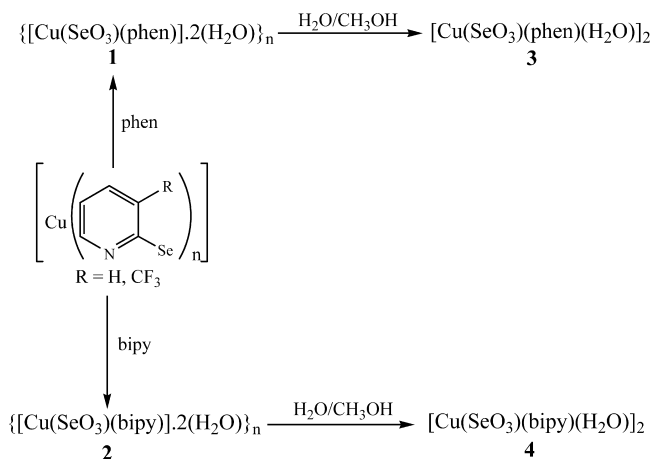
Cu(1)–N(2)	1.986(2)	Cu(1)–N(1)	1.992(2)
Cu(1)–N(4)	2.027(2)	Cu(1)–N(3)	2.031(2)
Cu(1)–O(3)	2.370(2)	O(1)–C(1)	1.252(3)
O(2)–C(7)	1.259(3)	N(1)–C(5)	1.350(4)
N(1)–C(1)	1.365(3)	N(2)–C(11)	1.341(3)
N(2)–C(7)	1.364(3)	N(3)–C(13)	1.332(3)
N(3)–C(17)	1.350(3)	N(4)–C(22)	1.336(3)
N(4)–C(18)	1.343(3)		
Hydrogen Bonds for 4 [Å and deg]			
D–H...A	d(D–H)	d(H...A)	d(D...A) <(DHA)>
O(3)–H(1A)...O(1)	0.87(4)	1.78(4)	2.605(4) 156(4)
O(3)–H(1B)...O(2) ^a	0.79(4)	2.17(4)	2.910(3) 158(4)

^a Symmetry transformations used to generate equivalent atoms: $x + 1, y, z$.

**Figure 1.** Compound 5.

The isolation of **5** provides a clue for the formation of the products. The first part of the reaction could involve oxidation of the selenium atom, followed by nucleophilic attack of H₂O on the C2 atom of the pyridine ring and the loss of SeO₃²⁻ to provide the final products.

The presence of CF₃ increases the sensitivity of C2 to nucleophilic attack, and the same experiments were therefore carried out using the copper derivative of 2-selenol pyridine to check if in this case the nucleophilicity of C2 was sufficiently high to produce the same result. In fact, the isolated compounds were the same as before. 2-Selenol pyridine is much cheaper than 3-trifluoromethyl-2-selenol pyridine, and the use of 2-selenol pyridine is therefore recommended. These results are summarized in Scheme 1.

Scheme 1

The IR spectra of complexes **1–5** show a broad band at about 3390 cm⁻¹ attributable to $\nu(\text{OH})$ stretching of water.

The spectra of **1–4** also show four bands that can be assigned to the coordinated selenite group.²³ The bands around 870 and 770 cm⁻¹ can be attributed to the non-degenerate symmetry stretching vibrations of the SeO₃²⁻ ion, and the most intense band at 740 cm⁻¹ is characteristic of the asymmetric stretching vibration of Se–O modes for selenides, and the other at 460 cm⁻¹ is assigned to the O–Se–O bending mode. In addition, the spectra of the phenanthroline (**1,3**) and bipyridine (**2,4**) complexes show bands around 1620, 1515, 850, and 720 cm⁻¹ for phen complexes and 760 and 729 cm⁻¹ for bipy complexes, and these are typical for coordinated phen and bipy.²⁴

Description of Structures. The complexes {[Cu(SeO₃)(phen)]·2(H₂O)}_n (**1**), {[Cu(SeO₃)(bipy)]·2(H₂O)}_n (**2**), [Cu(SeO₃)(H₂O)(phen)]₂·4H₂O (**3**), [Cu(SeO₃)(H₂O)(bipy)]₂·2H₂O (**4**), and [Cu(3-CF₃-pyO)₂(bipy)(H₂O)] (**5**) were studied by X-ray diffraction. The crystal parameters, experimental details for data collection and bond distances and angles for all these compounds are provided as Supporting Information.

Crystallization of the products from acetonitrile resulted in the formation of the polymeric species {[Cu(SeO₃)(phen)]·2(H₂O)}_n (**1**) and {[Cu(SeO₃)(bipy)]·2(H₂O)}_n (**2**), which have very similar structures and will therefore be discussed together. It is worth noting that the crystal network of compound **1** also contains half a molecule of acetonitrile (disordered) in the asymmetric unit, and this was removed from the network because of convergence problems. In any case, these solvent molecules occupy holes in the network and do not affect the final packing in the compound, as evidenced by comparison with compound **2**, which does not have any solvent molecule.

The dimeric species [Cu(SeO₃)(H₂O)(phen)]₂·4H₂O (**3**) and [Cu(SeO₃)(H₂O)(bipy)]₂·2H₂O (**4**) are also structurally very similar, and these will also be discussed together.

Structures of {[Cu(SeO₃)(phen)]·2(H₂O)}_n (1**) and {[Cu(SeO₃)(bipy)]·2(H₂O)}_n (**2**).** Perspective views of the molecular structures of **1** and **2** are shown in Figures 2a and 3 along with the atom labeling schemes used. Crystallographic data and a selection of bond distances and angles (with the estimated standard deviations) are given in Tables 2 and 3.

Each of the asymmetric units in compounds **1** and **2** contain a unique crystallographically distinct copper atom, a selenite anion, a phenanthroline molecule (in **1**) or a bipyridine (in **2**), and two water molecules that are not coordinated to the metal. In both compounds the copper atom is coordinated by two nitrogen atoms from the bidentate chelate ligand and by three oxygen atoms from three different selenite ligands to give an N₂O₃ environment for the metal. The geometry around the copper atom can be defined a

(23) Gopinath, A. B.; Devanarayanan, S.; Castro, A. *Spectrochim. Acta* **1998**, *54A*, 785–791.

(24) (a) Rodríguez, L.; Labisbal, E.; Susa-Pedrares, García-Vázquez, J. A.; Romero, J.; Durán, M. L.; Real, J. A.; Sousa, A. *Inorg. Chem.* **2006**, *45*, 7903–7914. (b) Beloso, I.; Castro, J.; García-Vázquez, J. A.; Pérez-Lourido, P.; Romero, J.; Sousa, A. *Polyhedron* **2006**, *25*, 2673–2682. (c) Beloso, I.; Castro, J.; García-Vázquez, J. A.; Pérez-Lourido, P.; Romero, J.; Sousa, A. *Inorg. Chem.* **2005**, *44*, 336–251. (d) Rodríguez, A.; Sousa-Pedrares, A.; García-Vázquez, J. A.; Romero, J.; Sousa, A. *Eur. J. Inorg. Chem.* **2005**, 2242–2254.

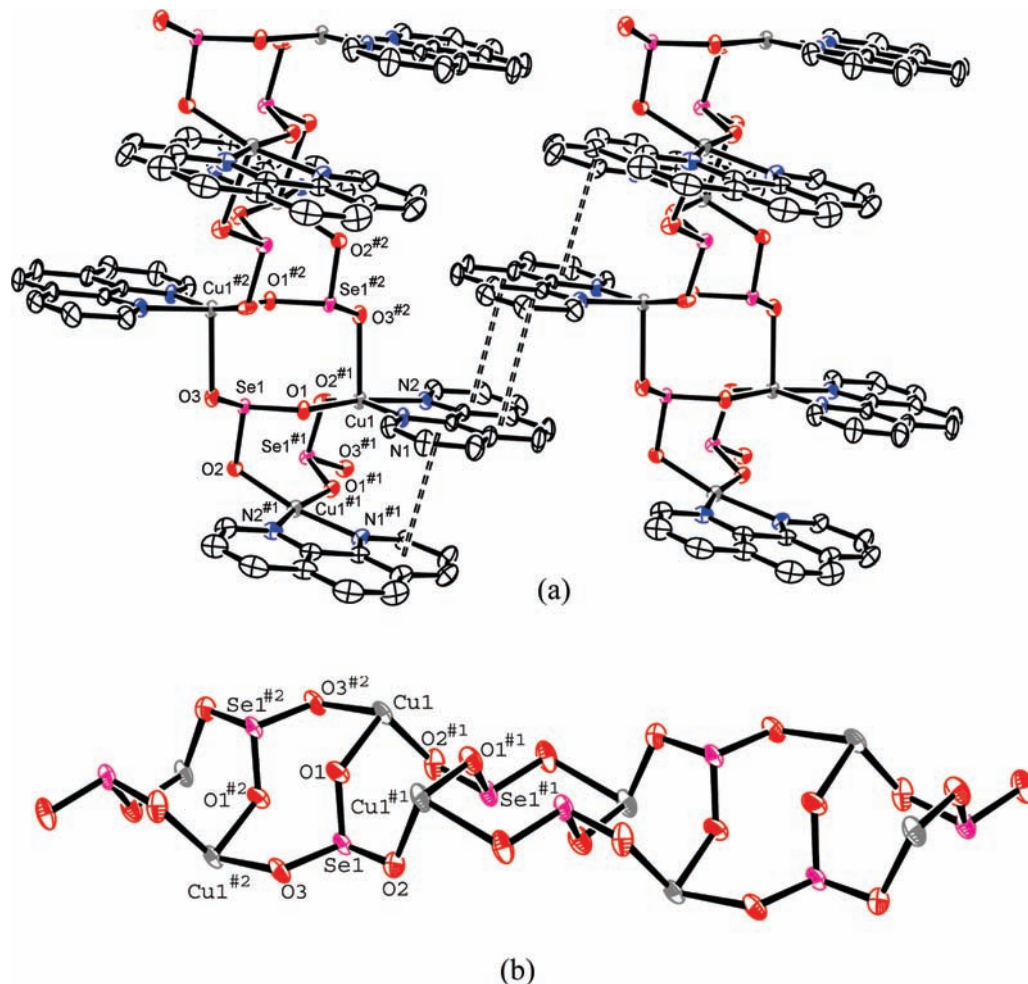


Figure 2. (a) Crystal packing diagram for **1**. Intermolecular and intramolecular π - π stacking interactions between phenanthroline rings are represented by dashed lines. (b) Partial view shows the strip of $\{[\text{Cu}(\text{SeO}_3)(\text{phen})] \cdot 2(\text{H}_2\text{O})\}_n$ (**1**).

square-based pyramid with a geometric parameter τ of 0.007 for **1** and 0.125 for **2**.²⁵ The base of the pyramid consists of two nitrogen atoms, N(1) and N(2), from the chelate ligand and two oxygen atoms [O(1) and O(2)^{#1}] from the two different selenite groups. The apical position is occupied by a more weakly bonded oxygen [O(3)^{#2}] from a third selenite group. The base of the pyramid is essentially planar [maximum deviation 0.062(2) Å for N(2) in **1** and 0.113(3) Å for N(1) in **2**], and in both compounds the copper atom is located slightly above this plane in the direction of the apical position [0.175(2) Å in **1** and 0.171(2) Å in **2**].

The selenite groups bridge three copper centers in an asymmetric manner and establish two strong interactions with two copper atoms, Cu(1) and the symmetry related Cu(1)^{#1}, with bond distances of 1.934(3) and 1.986(4) Å for **1** and 1.946(4) and 1.986(5) Å for **2**. These distances are similar to those found in other pentacoordinated copper complexes with oxygen donor ligands.²⁶ The third oxygen establishes a weaker interaction with a third copper atom Cu(1)^{#2}, which is related to Cu(1) through an inversion center. The bond length is 2.349(4) Å for **1** and 2.353(4) Å for **2** and, although

these are longer than the distances discussed above, they are shorter than the sum of the van der Waals radii, 2.8 Å.²⁷ The different energy of the Cu–O bonds is reflected in the Se–O bond distances in the selenite ligand, with values of 1.700(4) and 1.722(4) Å (**1**) and 1.711(4) and 1.707(4) Å (**2**) for those whose oxygen atoms are strongly bonded to the copper and shorter values, 1.667(3) Å (**1**) and 1.672(4) Å (**2**), for those with the oxygen weakly bonded to copper.

The existence of this weaker bond, Cu–O(apical), means that the structures of the polymers **1** and **2** can be considered as consisting of dimeric units $[\text{Cu}(\text{SeO}_3)(\text{phen})]_2$ or $[\text{Cu}(\text{SeO}_3)(\text{bipy})]_2$ that extend through weaker interactions involving the oxygen atoms in the positions apical to the two copper atoms (see Figure 2b). These dimeric polymerization units consist of eight-membered rings formed by Cu, O, and Se $[\text{Cu}(1)–\text{O}(1)–\text{Se}(1)–\text{O}(2)–\text{Cu}(1)^{\#1}–\text{O}(1)^{\#1}–\text{Se}(1)^{\#1}–\text{O}(2)^{\#1}]$ that contain a second order symmetry rotation axis and are in a boat conformation. The interactions between the copper atoms through the apical positions propagate the polymerization along the crystallographic *c* axis. This polymerization means that other eight-membered rings are formed between the connected dimeric units, and these are also formed by Cu, O, and Se $[\text{Cu}(1)–\text{O}(1)–\text{Se}(1)–\text{O}(3)–$

(25) Addison, A. W.; Rao, T. N.; Reedijk, J.; Van Rijn, J.; Verschoor, G. C. *J. Chem. Soc., Dalton Trans.* **1984**, 1349–1356.

(26) Labisbal, E.; García-Vázquez, J. A.; Romero, J.; Picos, S.; Sousa, A.; Castiñeiras, A.; Maichle-Mössner, C. *Polyhedron* **1995**, *14*, 663–670.

(27) Bondi, A. *J. Phys. Chem.* **1964**, *68*, 441–451.

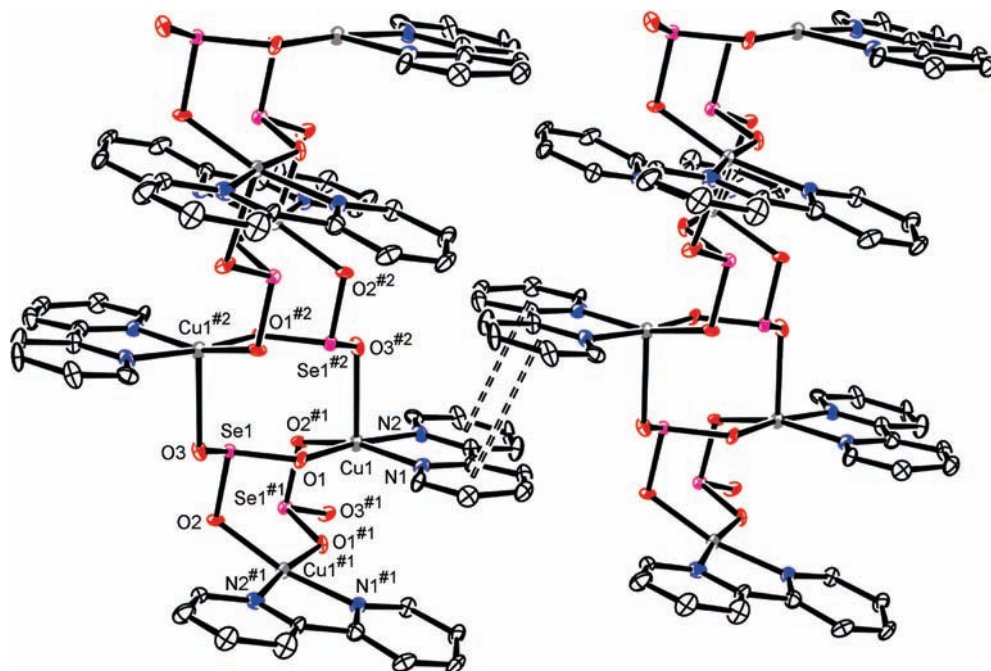


Figure 3. Crystal packing diagram of $\{[\text{Cu}(\text{SeO}_3)(\text{bipy})] \cdot 2(\text{H}_2\text{O})\}_n$ (**2**) showing the intramolecular π - π stacking interactions between bipyridine rings (represented by dashed lines).

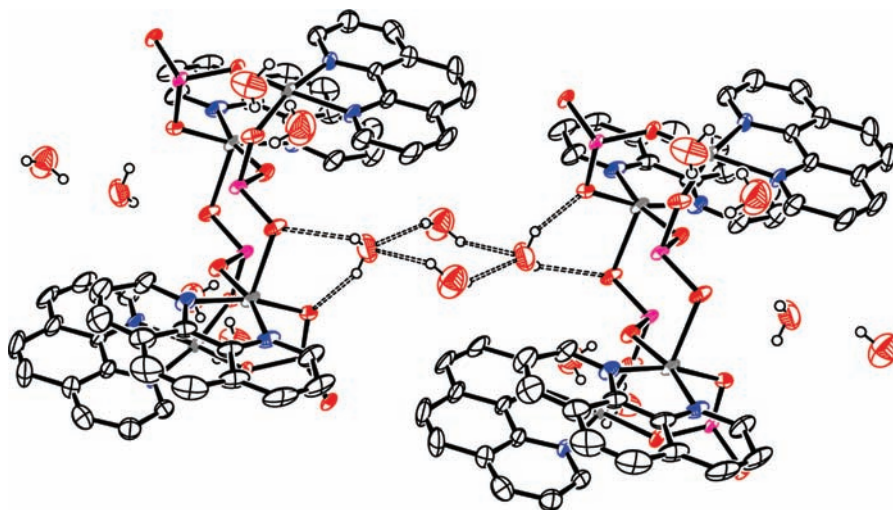


Figure 4. Hydrogen bonding in $\{[\text{Cu}(\text{SeO}_3)(\text{phen})] \cdot 2(\text{H}_2\text{O})\}_n$ (**1**). Dashed lines show the $\text{O}-\text{H} \cdots \text{O}$ interactions.

$\text{Cu}(1)^{\#2}-\text{O}(1)^{\#2}-\text{Se}(1)^{\#2}-\text{O}(3)^{\#2}$. These rings have an inversion center and are in a chair conformation. In this way, polymers **1** and **2** can both be described as a strip in which eight-membered rings with a boat conformation alternate with eight-membered rings in a chair conformation (Figure 2b). The phenanthroline rings in **1** and bipyridine rings in **2** are alternately located above and below the strip and are approximately parallel to the crystallographic AB plane (Figure 2a).

In the crystal packing in compounds **1** and **2** there are significant secondary π -stacking interactions between the rings of the phenanthroline units in **1** or bipyridine units in **2**, as well as hydrogen-bonding interactions between water molecules of crystallization and different groups on the ligands. The π -stacking interactions, which are mainly responsible for the overall crystal packing in the complexes, are different in the two complexes owing to the different number of aromatic rings that

are capable of forming this type of interaction. In both cases the interactions are established with other units with the same ligands from the same polymeric chain, as well as interactions with adjacent polymeric chains.

The interactions within the same polymer chain are within the interior of the dimeric building block $[\text{Cu}(\text{SeO}_3)(\text{NN})]_2$ (see Figures 2a and 3). Within these units the two ligands (NN) are related through a second order rotation axis, as indicated above. In both cases, this interaction involves the ring denoted $\text{N}(1)-\text{C}(1)-\text{C}(2)-\text{C}(3)-\text{C}(4)-\text{C}(5)$, and its symmetry equivalent in position #1 and this interaction is stronger for the phenanthroline ligands in compound **1** than for the bipyridine ligands in **2** (Figure 3). This situation is reflected in the distances between the centers of the rings, 3.471 Å in **1** and 3.839 Å in **2**. In this way, and according to the criterion proposed by Janiak,²⁸ which establishes the existence of interactions between parallel rings when their

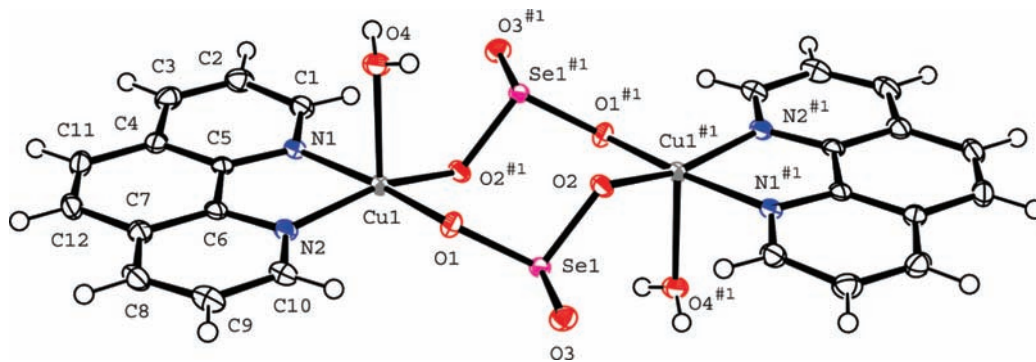


Figure 5. Structure of $[\text{Cu}(\text{SeO}_3)(\text{phen})(\text{H}_2\text{O})_2] \cdot 4\text{H}_2\text{O}$ (3).

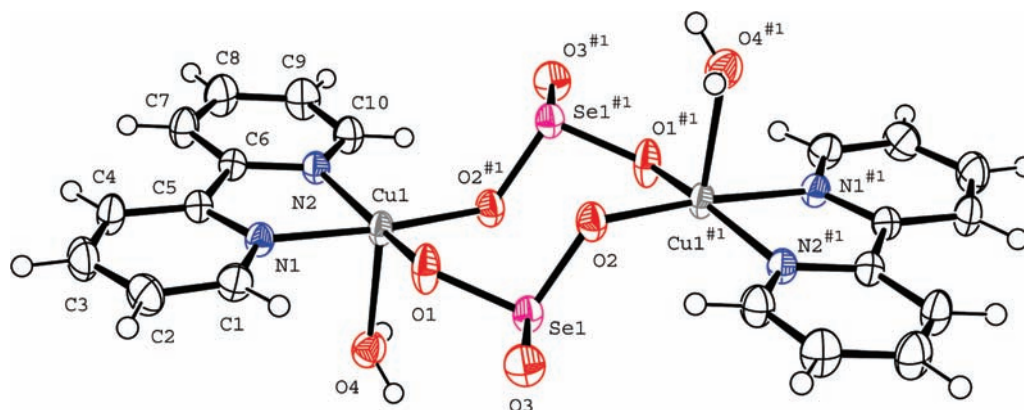


Figure 6. Structure of $[\text{Cu}(\text{SeO}_3)(\text{bipy})(\text{H}_2\text{O})_2] \cdot 2\text{H}_2\text{O}$ (4).

centroids are between 3.3 and 3.8 Å apart, it can be considered that interactions do not exist between the bipyridine ligands and, furthermore, that the position of the rings gives rise to a large dihedral angle, $16.28(22)^\circ$, a situation that is different to that found in compound **1**. In that case, in addition to having a lower distance between centroids, the aforementioned dihedral angle is much lower, $4.62(25)^\circ$. This interaction is of the *face to face* type, a situation that is not typical.

In both cases the interactions between adjacent polymer chains involve two aromatic rings (see Figures 2a and 3). In polymeric compound **1**, the aromatic rings involved in the interactions between chains are the two discussed above, which are not used for the interactions within the same chain. In the case of polymeric compound **2**, the rings involved are the two present in the bipyridine ligand. It is worth noting that in this case one of the rings is already involved in the interaction within the dimeric building block, meaning that this interaction is relatively weak compared to that in polymer **1**. As such, in this compound two equivalent π -stacking interactions are established; one between the ring denoted N(2)–C(6)–C(7)–C(8)–C(9)–C(10) and the symmetry equivalent through the central ring C(4)–C(5)–C(6)–C(7)–C(11)–C(12) in position #3, and another identical interaction between the central ring and the equivalent of the ring with N(2) in position #3. It is worth noting that the interaction is very effective, given that the rings are in a parallel disposition [angle between planes = $0.81(23)^\circ$] and are reasonably close to one another (3.583 Å). In addition,

the interactions are approximately *face to face*, identical to those occurring in the interactions within the same polymer chain.

In polymer **2** there are two equivalent π -stacking interactions; one between the ring containing N(1) and the symmetry equivalent of the ring with N(2) in position #3, and another identical interaction between the ring containing N(2) and the equivalent of the ring with N(1) in position #3 [Symmetry code #3: $-x - 1/2, -y - 1/2, -z$]. In this case, where such an interaction exists and it is also very close to a *face to face* arrangement, the interaction is less intense, a situation that is reflected in the distance between the two centroids (3.626 Å) and in the interaction geometry [angle between the rings = $7.45(27)^\circ$].

Polymers **1** and **2** both have two water molecules of crystallization per asymmetric unit. The bond distances and angles for the hydrogen bonding interactions involving the water molecules of crystallization are given in Tables 2 and 3. The water molecules of crystallization interact with each other through hydrogen bonding and also interact with different groups in the same polymer chain (see Figure 4). In both compounds the oxygen of one of the water molecules, O(1s), establishes two hydrogen bonding interactions with two oxygen atoms in the same coordination sphere of each copper center; O(2) in the basal plane and O(3)^{#4} in the apical position. The oxygen of the second water molecule, O(2s), establishes weaker interactions with the oxygen of the water molecule O(1s) and its symmetry equivalent O(1s)^{#5}. Each of these water molecules O(1s) interacts with a polymer chain in such a way that the second water molecules O(2s) weakly

(28) Janiak, C. *J. Chem. Soc., Dalton Trans.* **2000**, 3885–3896.

connect adjacent polymer chains to one another. As discussed below, the interactions that are ultimately responsible for the relative orientation of the polymer chains, as well as the crystal packing arrangements in compounds **1** and **2**, are the π -stacking interactions.

Structures of [Cu(SeO₃)(phen)(H₂O)]₂·4H₂O (3**) and [Cu(SeO₃)(bipy)(H₂O)]₂·2H₂O (**4**).** Crystallization of polymers **1** and **2** from 1:1 methanol/water mixtures gives rise to the formation of dimeric species **3** and **4**. Perspective views of the molecular structures of **3** and **4** along with the atom labeling schemes used are shown in Figures 5 and 6. Crystallographic data and a selection of bond distances and angles (with the estimated standard deviations) are given in Tables 4 and 5.

Dissolution of polymers **1** and **2** in the presence of excess water leads to the breakdown of the weaker apical interactions, which in turn gives rise to the formation of the dimeric compounds **3** and **4**. In these compounds the selenite groups only establish bridges between two Cu atoms, Cu(1) and its symmetry equivalent Cu(1)[#], through two of their oxygen atoms, O(1) and O(2). The third oxygen atom remains uncoordinated, O(3).

The coordination environments of the copper atoms are very similar to those found in **1** and **2**. Each metal center has a coordination number 5 through coordination to the two nitrogens of the corresponding nitrogenated coligand, N(1) and N(2), to two equivalent oxygen atoms of different selenite groups, O(1) and O(2)[#], and to the oxygen of a water molecule, O(4). As in compounds **1** and **2**, the coordination geometry can be described as a square-based pyramid ($\tau = 0.158$ in **3** and 0.185 in **4**), in which the nitrogens of the bidentate ligand and the two oxygen atoms of the selenite groups occupy the base of the pyramid and the oxygen of the water molecule occupies the apical position. The base of the pyramid is essentially planar [maximum deviation 0.168(1) Å, N(2), for **3** and 0.084(1) Å, N(1), for **4**]. In both compounds the copper atom is slightly above the plane in the direction of the apical position, 0.147(1) Å for **3** and 0.137(1) Å for **4**.

The Cu–O distances in the basal plane, 1.9341(16) and 1.9633(16) Å in **3** and 1.9229(19) and 1.9482(19) Å in **4**, are typical and are very similar to values found in the same plane in compounds **1** and **2** (vide supra). Once again this coordination is reflected in the corresponding Se–O distances. The oxygen atoms bonded to the copper, O(1) and O(2), give rise to Se–O distances of 1.7054(16) and 1.7179(16) Å for **3** and 1.6922(19) and 1.711(2) Å for **4**, while the Se–O(3) distance, which involves a non-bonded oxygen atom, is shorter: 1.6718(17) Å in **3** and 1.6641(19) Å in **4**. The Cu–O apical bond distances, 2.2613(19) and 2.317(2) Å in **3** and **4**, respectively, are relatively high. Normally, the Cu–O_w bond distances in pentacoordinated copper complexes are much longer than the bonds in the basal plane, as found in the case of pentacoordinated copper(II) complexes containing both nitrogen and oxygen donor atoms.²⁹

As in compounds **1** and **2**, the dimeric compounds contain eight-membered rings formed by Cu, O, and Se atoms [Cu(1)–O(1)–Se(1)–O(2)–Cu(1)[#]–O(1)[#]–Se(1)[#]–O(2)[#]]. The main difference between the dimeric building blocks in the polymeric

compounds **1** and **2** and the dimers **3** and **4** is that in the latter the rings have inversion symmetry and are in a chair conformation.

In the crystal packing of compounds **3** and **4** the dimeric species are arranged in such a way that the π -stacking interactions between aromatic rings are favored. All of the aromatic rings of the nitrogenated ligands are involved in this type of interaction. In an analogous way to compounds **1** and **2**, the differences observed for this type of interaction concern the number of aromatic rings present in the corresponding ligands. As can be seen in Figure 7, the rings in each nitrogenated ligand establish a π -stacking interaction with another symmetry equivalent ligand located below the base of the square pyramid. In both cases the ring containing N(1) interacts with the symmetry equivalent in position #2 of the ring containing N(2), while the ring containing N(2) interacts in an identical manner with the equivalent in #2 of the ring with N(1). It is worth noting that these interactions are *face to face* in nature and involve almost perfect alignment, a situation that is relatively rare.²⁸ In compound **3** the central phenanthroline ring establishes another π -stacking interaction with a symmetry equivalent ring located above the base of the square pyramid in the equivalent position #3. In this case it is worth noting the low value of the centroid-centroid distance, 3.419 Å, which provides evidence of a strong interaction according to the criterion proposed by Janiak. In contrast to the interaction below the basal plane, this interaction is an *offset or slipped stacking*, that is, *the rings are parallel displaced*.

In compound **4** the aromatic rings of the bipyridine ligand in the unit located above the base are sufficiently distant to establish a π -stacking interaction (centroid-centroid distance 4.646 Å). In dimer **3** the distance between the nitrogenated phenanthroline rings and those in the equivalent position #3 (above the base plane) is 4.632 Å, which is almost identical to that found in **4**, showing that the most important interaction occurs with the group located below the base plane.

In compounds **3** and **4** hydrogen-bonding interactions occur that involve water molecules of crystallization. There are essentially two types of interaction: those in the same direction as the stacking interactions, which connect the dimeric units through water molecules, and those perpendicular to the stacking interaction, which connect the dimeric units through the uncoordinated oxygen atoms of the selenite ligands.

The stacking interactions generate holes between the dimers, and all of the water molecules are accommodated within these holes in both compounds. All but one of these water molecules establish hydrogen-bonding interactions in the same direction as the stacking interactions, and these are established with the coordinated water molecules and

(29) (a) Beloso, I.; Borrás, J.; Castro, J.; García-Vázquez, J. A.; Pérez-Lourido, P.; Romero, J.; Sousa, A. *Eur. J. Inorg. Chem.* **2004**, 635–645. (b) Chapman, R. L.; Stephens, F. S.; Vagg, R. S. *Inorg. Chim. Acta* **1980**, *43*, 29–33. (c) Mulqi, M.; Stephens, F. S.; Vagg, R. S. *Inorg. Chim. Acta* **1981**, *51*, 9–14. (d) Stephens, F. S.; Vagg, R. S. *Inorg. Chim. Acta* **1982**, *57*, 43–49. (e) Mulqi, M.; Stephens, F. S.; Vagg, R. S. *Inorg. Chim. Acta* **1981**, *52*, 177–182.

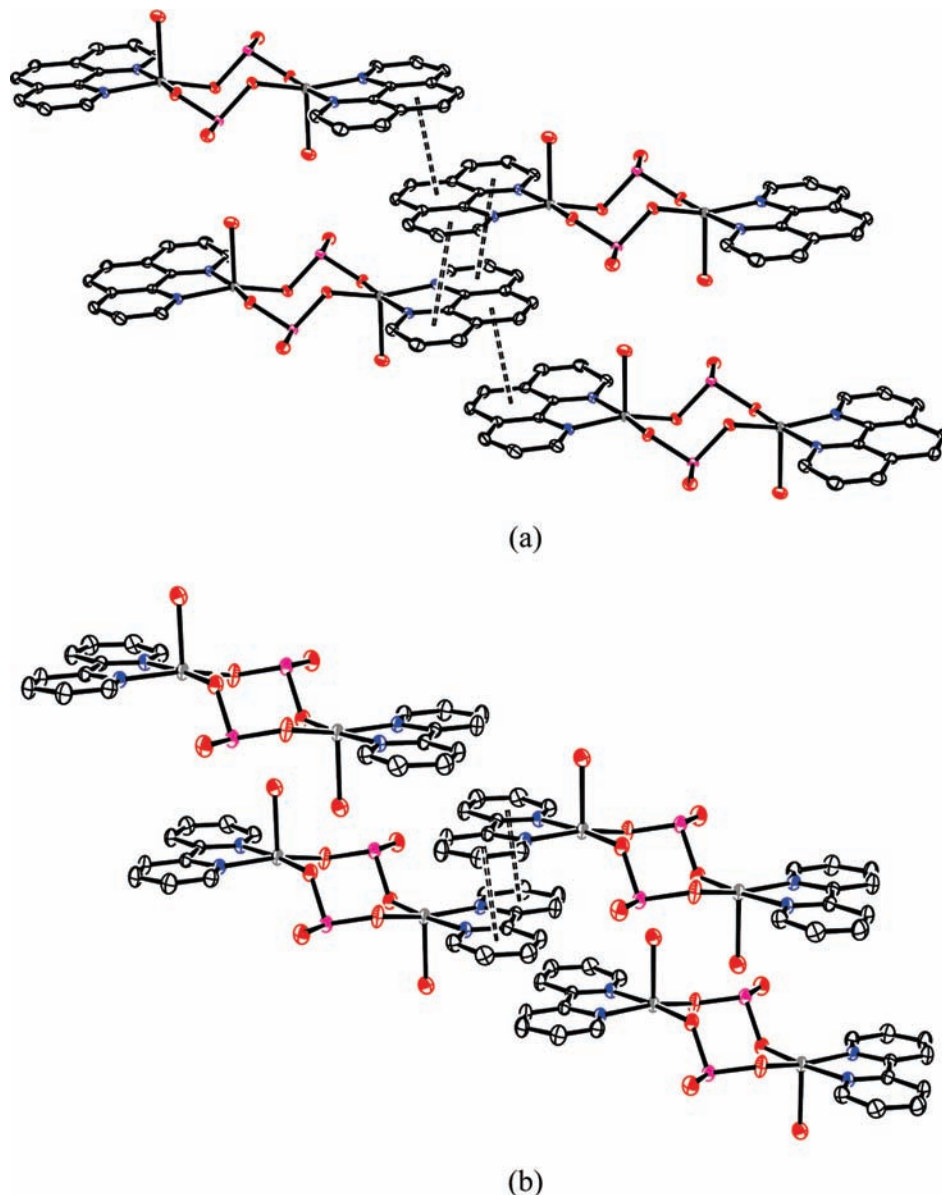


Figure 7. Crystal packing diagram (a) of $[\text{Cu}(\text{SeO}_3)(\text{phen})(\text{H}_2\text{O})]_2 \cdot 4\text{H}_2\text{O}$ (**3**) and (b) of $[\text{Cu}(\text{SeO}_3)(\text{bipy})(\text{H}_2\text{O})]_2 \cdot 2\text{H}_2\text{O}$ (**4**). The intramolecular π - π stacking interactions between phenanthroline (**3**) or bipyridine (**4**) rings are represented by dashed lines.

the non-coordinated oxygen atoms of the selenite groups coordinated to the metal. In this way the intermolecular interactions in this direction are reinforced (Tables 4 and 5). In compound **3** these interactions involve three water molecules whereas in **4** only one water molecule is involved. Given that the crystal packing is similar in both compounds, the conclusion that the stacking interactions dictate the orientation of the dimers is supported, and the hydrogen-bonding simply reinforces these stacking interactions.

One water molecule [O(1s)] is involved in hydrogen-bonding interactions in both compounds. In this case the bonding is perpendicular to the stacking interactions and connects dimeric units through the uncoordinated oxygen atoms of the selenite groups, as shown in Figure 8. These interactions are strong (see Tables 4 and 5) and are responsible for the crystal packing in this direction.

Structure of $[\text{Cu}(\text{3-CF}_3\text{-pyO})_2(\text{bipy})(\text{H}_2\text{O})]$ (5**).** A perspective view of the molecular structure of **5** is shown in Figure 9 along with the atom labeling scheme used. Crystallographic data and a selection of bond distances and angles (with the estimated standard deviations) are given in Table 6.

The structure of compound **5** consists of neutral monomeric molecules in which the copper atom is coordinated by two 3- CF_3 -pyO ligands, which are bonded to the metal through the nitrogen atoms by two nitrogens of the bipyridine ligand and by the oxygen atom of a water molecule. The environment around the metal is square-pyramidal ($\tau = 0.135$). The base of the pyramid is essentially planar [maximum deviation 0.086(1) Å, N(3)] and is defined by the four nitrogen atoms. The copper is located 0.185(1) Å above the plane in the direction of the apical oxygen atom of the water molecule.

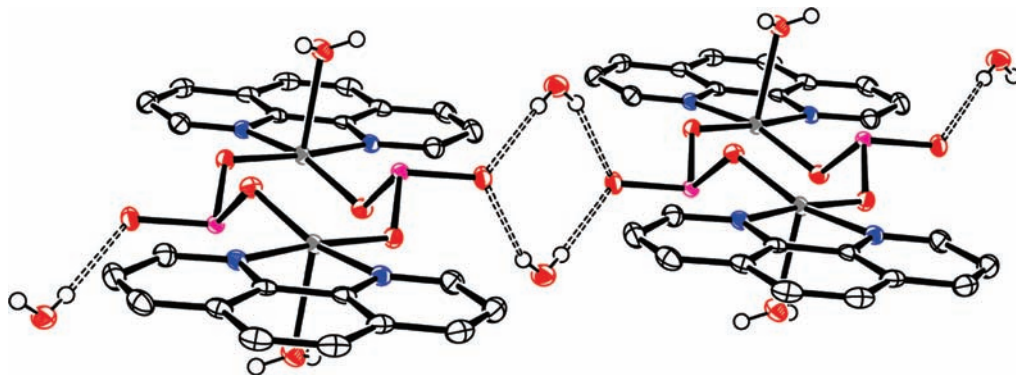


Figure 8. Hydrogen bonding in $[\text{Cu}(\text{SeO}_3)(\text{phen})(\text{H}_2\text{O})]_2 \cdot 4\text{H}_2\text{O}$ (**3**). Dashed lines show the $\text{O}-\text{H}\cdots\text{O}$ interactions.

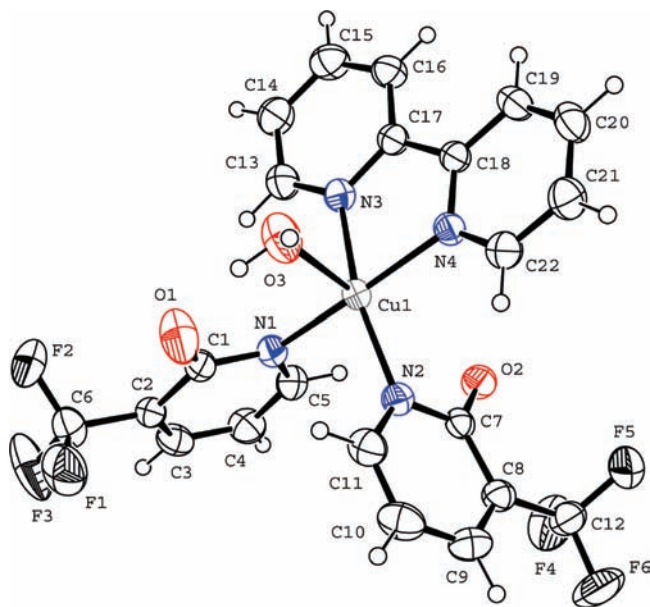


Figure 9. Structure of $[\text{Cu}(3\text{-CF}_3\text{-pyO})_2(\text{bipy})(\text{H}_2\text{O})]$ (**5**).

The Cu–N bond lengths, 1.986(2)–2.031(2) Å, are in the normal range found for Cu–N(py) bonds³⁰ and are very similar to those in compounds **1**–**4**. The Cu–O distance, 2.370(2) Å, is also similar to those found in dimers **3** and **4**, 2.2613(19) and 2.317(2) Å.

The anionic 3- CF_3 -pyO ligand is coordinated to the copper in the lactam form, as evidenced by the C–O bond distances, 1.252(3) and 1.259(3) Å, which are characteristic of a double bond. The C–C distances in the two 3- CF_3 -pyO ligands are different and correspond to single and double bonds (see Supporting Information).

In this compound, in contrast to the situation found in the compounds described above, π -stacking between the ligand rings is not observed. Hydrogen-bonding interactions are observed in **5**, and these are responsible for the crystal packing. These interactions involve the coordinated water molecule, and $\text{F}\cdots\text{F}$ interaction between the $-\text{CF}_3$ groups are also evident. An intramolecular interaction is observed between the coordinated water molecule and O(1) of a 3- CF_3 -pyO ligand, along with an intermolecular interaction between

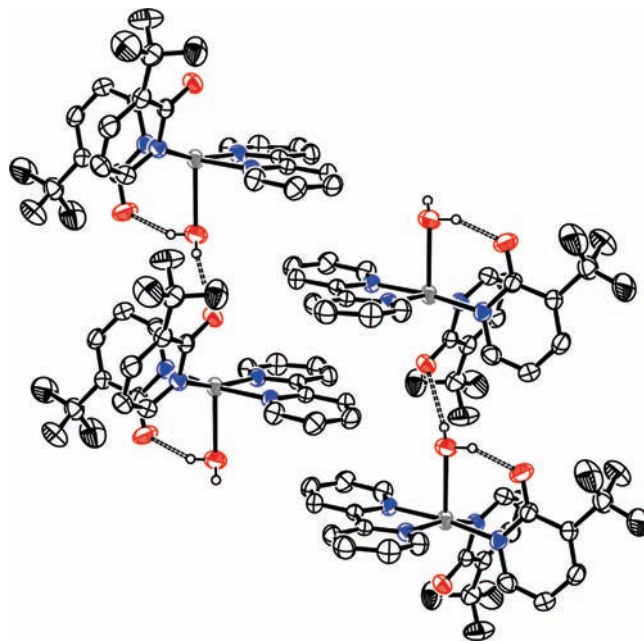


Figure 10. Hydrogen bonding in $[\text{Cu}(3\text{-CF}_3\text{-pyO})_2(\text{bipy})(\text{H}_2\text{O})]$ (**5**). Dashed lines show the $\text{O}-\text{H}\cdots\text{O}$ interactions.

O(2) of the other ligand in the equivalent position #1. This intermolecular interaction connects the molecules along the crystallographic a axis, as shown in Figure 10. It can be seen that the bipyridine ligands are arranged parallel along the crystallographic a axis, although the distances between centroids are sufficiently high that the existence of π -stacking interactions can be ruled out. The disposition of the molecules is such that the CF_3 groups are oriented toward other trifluoromethyl groups, with distances between the fluorine atoms in the range 2.65–3.52 Å. This type of interaction has been reported previously for other complexes containing these groups,³¹ and they play an important role in the crystal packing of other heteroleptic complexes.

Magnetic Properties. The magnetic behavior of complexes **1** and **3** expressed in the form of $\chi_M T$ (**1**) or χ_M (**3**) versus T , where χ_M is the molar magnetic susceptibility and T the temperature, is shown in Figure 11. In the temperature region 300–60 K, $\chi_M T$ has a value close to 0.425 $\text{cm}^3 \text{K mol}^{-1}$, which is the expected value for magnetically uncoupled Cu(II) ions ($g \approx 2.13$). At temperatures below 60

(30) (a) Gavioli, G. B.; Borsari, M.; Menabue, L.; Saladini, M. *J. Chem. Soc., Dalton. Trans.* **1991**, 2961–2963. (b) Otter, C. A.; Couchman, S. M.; Jeffery, J. C.; Mann, K. L. V.; Psillakis, E.; Ward, M. D. *Inorg. Chim. Acta* **1998**, 278, 178–184.

(31) Halper, S. R.; Cohen, S. M. *Angew. Chem., Int. Ed.* **2004**, 43, 2385–2388.

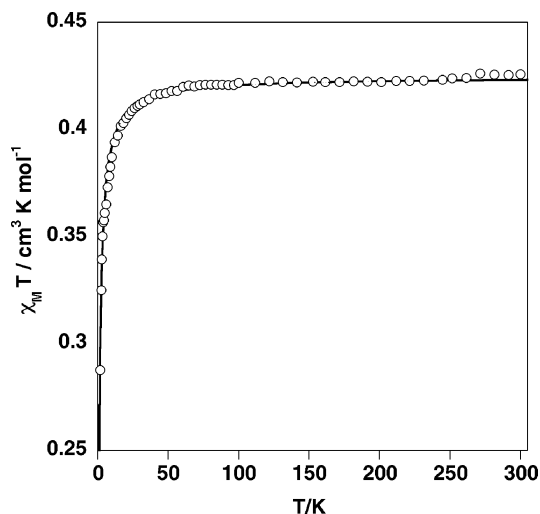


Figure 11. $\chi_M T$ versus T plot for compound **1**. The solid line represents the best fit to the experimental data (see text).

K, $\chi_M T$ decreases more markedly down to $0.287 \text{ cm}^3 \text{ K mol}^{-1}$ at 2 K. This behavior is reminiscent of compounds displaying very weak intramolecular antiferromagnetic coupling. Consequently, a maximum was not observed in the χ_M versus T plot.

Taking into account the crystal structure of **1**, that is, an infinite one-dimensional chain, we analyzed these magnetic data using Bonner and Fishers' expression (1):³²

$$\chi = \frac{Ng^2\beta^2}{kT} \frac{0.25 + 0.074975x + 0.075235x^2}{1.0 + 0.9931x + 0.172135x^2 + 0.757825x^3} \quad (1)$$

where $x = |J|/kT$, deduced from the Hamiltonian $H = -J\sum_i S_{Ai} S_{Ai+1}$. J expresses the intramolecular exchange interaction, S_A is the quantum spin operator, and N , β , g , and T have their usual meanings. A least-squares fit of the data through eq 1 leads to the values of $J = -0.9 \text{ cm}^{-1}$, $g = 2.12$, and $R = 4.6 \times 10^{-5}$. R is the agreement factor defined as $\sum_i [(\chi_M)_i^{\text{exptl}} - (\chi_M)_i^{\text{calc}}]^2 / [(\chi_M)_i^{\text{exptl}}]^2$.

The magnetic behavior of **2** is very similar to that of **1**, as expected given that they have the same structure (see SM). The most prominent difference is due to the α -diimine organic ligand 2,2'-bipy and phen coordinated to the copper(II) ion. The fit of the experimental and calculated data gives $J = -0.6 \text{ cm}^{-1}$, $g = 2.17$, and $R = 2 \cdot 10^{-4}$ for **2**.

The χ_M versus T plot for **3** shows a continuous increase from $2.77 \times 10^{-3} \text{ cm}^3 \text{ mol}^{-1}$ up to a maximum of $1.98 \times 10^{-2} \text{ cm}^3 \text{ mol}^{-1}$ at 20 K. The value then decreases at lower temperatures and reaches a value of $3.06 \times 10^{-3} \text{ cm}^3 \text{ mol}^{-1}$ at 5 K (Figure 12). According to the molecular structure of **3** the experimental data were analyzed through the spin-only formalism for a dimeric species involving an isotropic Heisenberg interaction with $S_A = 1/2$: $H = -JS_A S_A$. The resulting χ_M versus T expression deduced from this Hamiltonian is the so-called Bleaney–Bowers expression, which has been implemented to take account of

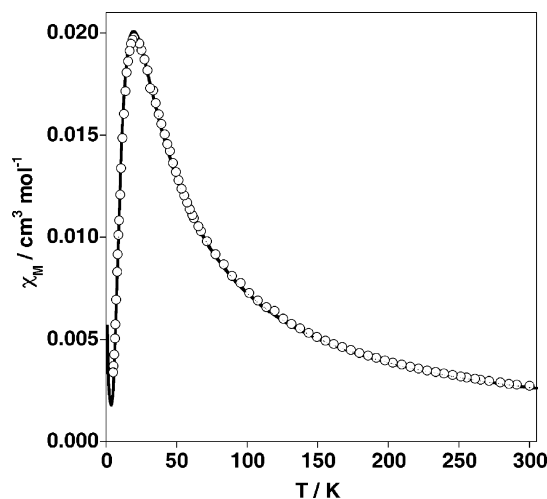


Figure 12. χ_M versus T plot for compound **3**. The solid line represents the best fit to the experimental data (see text).

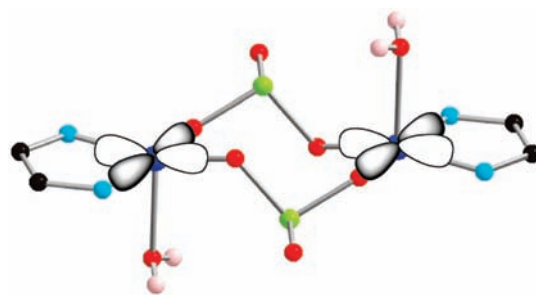


Figure 13. Schematic view of the dinuclear species displaying the relative position of the $d(xy)$ -type orbitals.

paramagnetic impurities and temperature-independent paramagnetism.³³

$$\chi_M = (1 - \rho) \left(\frac{2N\beta^2 g^2}{kT} [3\exp(J/kT)]^{-1} \right) + \rho \frac{N\beta^2 g^2}{2kT} + N\alpha \quad (2)$$

The parameters J , g , and ρ (percentage of paramagnetic impurities) were determined by least-squares fit minimization. The best fit for calculated and experimental χ_M values was found for $J = -22.1 \text{ cm}^{-1}$, $g = 2.07$, $\rho = 0.01$, $N\alpha = 108 \times 10^{-6} \text{ cm}^3 \text{ mol}^{-1}$, and $R = 7 \times 10^{-4}$. Although it was not possible to obtain the experimental χ_M versus T data for compound **4**, it is expected to be essentially the same as described for **3**, since their molecular structures are very similar.

The value of the coupling constant for these derivatives is rather small but is consistent with previous data.³⁴ In the dinuclear species' **3** and **4**, the molecular orbital bearing the unpaired electron is essentially of $d(x^2 - y^2)$ symmetry, which is situated in the plane of the equatorial coordination sphere around the copper ions and is defined by the shortest Cu–N and Cu–O bond distances. Consequently, the spin density is partially delocalized on the equatorial ligands. The two $d(x^2 - y^2)$ orbitals overlap through doubly connected selenite bridges [Cu···Cu separation $5.142(1) \text{ \AA}$, **3**] (see Figure 13).

(33) Kahn, O. *Molecular Magnetism*; VCH: New York, 1993.

(34) Larrañaga, A.; Mesa, J. L.; Pizarro, J. L.; Peña, A.; Olazcuaga, R.; Arriortua, M. I.; Rojo, T. *J. Solid State Chem.* **2005**, *178*, 3686–3697.

(32) Bonner, J. C.; Fischer, M. E. *Phys. Rev. A* **1964**, *135*, 640.

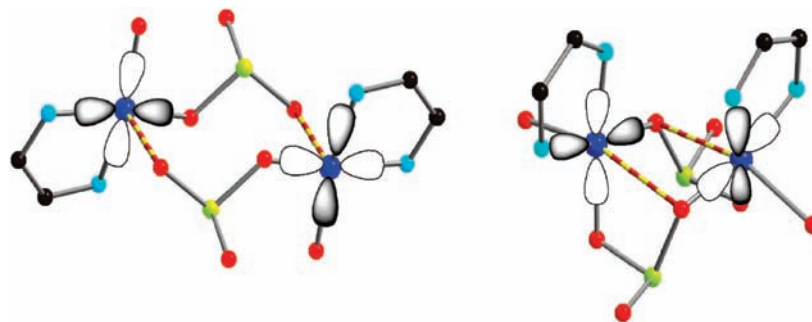


Figure 14. Schematic view of the two dinuclear “chair” and “boat” fragments displaying the relative position of the $d(xy)$ -type orbitals. Yellow-red bonds represent the long Cu–O semi-coordinative bonds.

However, despite this favorable relative orientation of the $d(x^2-y^2)$ orbitals, the selenite sp^3 molecular orbital enables a very small overlap between them and hence a reduced value for the magnetic interaction is observed. As far as we know, examples of selenite-bridged dinuclear complexes have not been reported until now. A possible comparison could be made with respect to sulfato-bridged compounds, although in most of these compounds the sulfato ion is part of a bridging network consisting of different ligands, which makes it very difficult to deduce the contribution arising from the magnetic pathway through the sulfate.³⁵ In this respect, Hatfield and co-workers reported the structure and magnetic characterization of $[\text{Cu}(\text{oaoH}_2)(\text{H}_2\text{O})(\text{SO}_4)]_2$ (oaoH_2 = oxamide oxime), a pure double-bridged SO_4^{2-} dinuclear compound.³⁶ The J value obtained for this compound, -2.55 cm^{-1} , is almost 10 times smaller than the one obtained for **3**. It is likely that the main reason for this difference is the coordination mode of the μ -sulfato ligands that connect the two copper ions through a short and a long Cu–O(SO_3) distance (vide infra).

As far as the chain compounds **1** and **2** are concerned, the J value deduced from the fit represents a resultant value arising from of two distinct magnetic pathways, which repeat alternately along the chain. One corresponds to the chair shaped $[\text{Cu}-\text{O}-\text{S}-\text{O}-\text{Cu}]_2$ pathway [$\text{Cu}\cdots\text{Cu}$ separation $5.226(1) \text{ \AA}$] similar to that shown for the dinuclear species but with a much more unfavorable orientation of the $d(x^2-y^2)$ orbitals (Figure 14, left). Indeed, the copper atoms are connected by a selenite anion through one short equatorial, Cu–O = $1.938(4) \text{ \AA}$, and one long axial, Cu–O = $2.350(4) \text{ \AA}$, distance in this chair conformation. Therefore, the two

symmetry related halves of the dimer interact with each other through a $d(z^2)$ -type orbital, which practically does not contain any electron spin density, and hence its contribution to magnetic exchange is expected to be insignificant. In the boat conformation [$\text{Cu}\cdots\text{Cu}$ separation $3.480(1) \text{ \AA}$] the $d(x^2-y^2)$ orbitals are almost parallel to each other, but the connectivity through the bridge is similar to that observed in **3** and **4**. Furthermore, the fact that the two halves of this fragment of the chain are practically face-to-face determines the occurrence of two long Cu–O distances, $2.720(4) \text{ \AA}$ (Figure 14, right). This monatomic exchange pathway is characterized by a Cu–O–Cu angle equal to $95.3(1)^\circ$ and clearly indicates the possible occurrence of very weak intramolecular ferromagnetic coupling. Almost total cancellation of the antiferro- and ferro-magnetic contributions would justify the reduced value for the experimental magnetic coupling observed for **1** and **2**.

Conclusions

Starting from $[\text{Cu}(\text{R-pySe})]$, a new series of heteroleptic selenites of copper (II), **1–4**, have been prepared. This procedure is milder than the hydrothermal method generally used to prepare this type of complexes.

The compounds **1** and **2** show a polymer structure and a weak antiferromagnetic coupling. Compounds **3** and **4** are obtained by recrystallization of **1** and **2** in a methanol–water (1:1) mixture. These compounds have a dinuclear structure with an antiferromagnetic coupling.

Acknowledgment. This work was supported by the Xunta de Galicia (Spain) (grant PGIDIT07PXIB203038PR) and by the Ministerio de Ciencia and Tecnología (Spain) (Grants CTQ2006-05298BQU and CTQ2007-64727-FEDER).

Supporting Information Available: Crystallographic data in cif format. This material is available free of charge via the Internet at <http://pubs.acs.org>.

IC8019099

- (35) (a) van Koningsbruggen, P. J.; Gatteschi, D.; de Graaff, R. A. G.; Haasnoot, J. G.; Reedijk, J.; Zanchini, C. *Inorg. Chem.* **1995**, *34*, 5175–5182. (b) Knuutila, P. *Inorg. Chim. Acta* **1982**, *58*, 201–206. (c) Thomson, L. K.; Hanson, A. W.; Ramaswamy, B. S. *Inorg. Chem.* **1984**, *23*, 2459–2465. (d) De Munno, G.; Julve, M.; Lloret, F.; Cano, J.; Caneschi, A. *Inorg. Chem.* **1995**, *34*, 2048–2053. (e) Kawata, S.; Kitagawa, S.; Enemoto, M.; Kumagai, H.; Katada, M. *Inorg. Chim. Acta* **1998**, *283*, 80–90.
- (36) Endres, H.; Nöthe, D.; Rossato, E.; Hatfield, W. E. *Inorg. Chem.* **1984**, *23*, 3467–3473.